Journal of Petroleum Science and Engineering 145 (2016) 205–212

Contents lists available at ScienceDirect

Journal of Petroleum Science and Engineering

journal homepage: www.elsevier.com/locate/petrol

Rock physics-based carbonate pore type identification using Parzen classifier

Amir Mollajan*, Hossein Memarian

School of Mining Engineering, University College of Engineering, University of Tehran, Tehran, Iran

ARTICLE INFO

Article history:
Received 16 May 2015
Received in revised form
16 January 2016
Accepted 30 March 2016
Available online 31 March 2016

Keywords:
Rock physics
The frame flexibility factor (γ)
Velocity Deviation Log (VDL)
Parzen classifier
Iran

ABSTRACT

Seismic velocity variation in carbonate rocks is a complicated function of different parameters such as mineral composition, porosity, pore type, saturation, and pore pressure. Among all, pore type is the main factor that affects reservoir permeability heterogeneity and change the velocity–porosity relationship. In this paper, a rock physics-based algorithm is presented to quantitatively identify three dominant pore types in a carbonate reservoir. The proposed algorithm is applied on data related to three wells drilled in a carbonate reservoir, southwest of Iran. We used the frame flexibility factor (γ), P-wave velocity–porosity and S-wave impedance–porosity trends as inputs of Parzen classifier to identify predominate pore type characterized by velocity-deviation log (VDL) in each depth. The results show that the proposed algorithm has high precision in classifying identified pore types with average accuracy of 76.7% throughout studied oil field.

1. Introduction

More than 50% of the world's oil and gas reserves are held within carbonate reservoirs (Dou et al., 2011). Carbonate reservoirs are identified by significant heterogeneity at numerous scales ranging from micro-scale, to giga scale which makes their characterization difficult. Geophysical applications in carbonate reservoirs are less mature and less abundant than those of siliciclastic reservoirs (Mahbaz et al., 2012). In carbonate rocks, the complex processes of sedimentation and diagenesis produce microporous grains and different pore sizes that occur at all scales of observation and measurement, resulting in a wide range of sonic wave velocity, in which compressional-wave velocity (V_P) ranges from 1700 to 6600 m/s and shear-wave velocity (V_S) from 600 to 3500 m/s (Eberli et al., 2003). Heterogonous pore system in carbonate rocks is due to some post-depositional processes such as physical transport, chemical alteration, dissolution and diagenesis (Anselmetti and Eberli, 1999; Assefa et al., 2003; Eberli et al., 2003; Adam et al., 2006; Baechle et al., 2009). Complex depositional and diagenetic processes form a variety of pore types by dissolution of components such as moldic pores, fenestral pores, intraparticle pores, vugs, etc. For a given mineral composition and fluid type, variation in pore types may affects reservoir permeability heterogeneity and dramatically change the acoustic wave velocity reveal that sonic wave velocity is a function not only of total porosity, but also of the predominant pore type (Anselmetti and Eberli, 1999; Dou et al., 2011; Wang et al., 2015). As a consequence, to successfully characterize carbonate reservoir rocks, it is essential to develop a robust rock physics model capable of handling various geological factors which affect acoustic properties of these rocks (Xu and Payne, 2009; Avseth et al., 2010).

Many works have been carried out to evaluate carbonate rock pore type complexity and propose a practical frame work for carbonate reservoir characterization (Bracco Gartner et al., 2005; Xu and Payne, 2009; Fournier et al., 2011; Pyrcz and Deutsch, 2014; Matonti et al., 2014).

The present study is aimed to propose a data-driven algorithm combined with rock physics modeling to identify three desired pore types quantitatively. We use data related to three wells drilled in a carbonate reservoir located in an oil field, southwest of Iran. To characterize the predominate pore types in each well the velocity-deviation is calculated by combining the sonic log with the neutron-porosity log. The frame flexibility factor (γ), P-wave velocity–porosity, and S-wave impedance–porosity trends are used to quantify the effect of pore structure on acoustic properties of studied reservoir. Finally, Parzen classifier is employed to identify predominate pore types in each depth.

2. Geological setting

The studied oil field is located in Khuzestan province, in the Abadan Plain area, southwest of Iran (Fig. 1). The Sarvak Formation with Cenomanian in age (Upper Albian to Upper Turonian) is the

* Corresponding author.
E-mail addresses: a.mollajan@ut.ac.ir (A. Mollajan), memarian@ut.ac.ir (H. Memarian).

http://dx.doi.org/10.1016/j.petrol.2016.03.021
0920-4105/

Nomenclature

VDL	Velocity-deviation log
CCR	Classification Correctness Rate
XRD	X-Ray Diffraction
γ	Frame flexibility factor
V_p	P-wave velocity
V_s	S-wave velocity
SI	Shear Impedance
RHOB	Density log
GR	Gamma ray
NPHI	Neutron density log
NIOC	National Iranian Oil Company
K_s	Matrix bulk modulus
K_f	Fluid bulk modulus
ϕ	Porosity
h	Parzen window

main carbonate reservoir unit in this structure. This formation is a part of Bangestan group which includes Kazhdumi, Sarvak, Surgah and Ilam Formation (Bashari 2007a).

Fig. 2 shows a simplified stratigraphy of the Cretaceous. According to the figure, in Abadan plain an argillaceous unit (Laffan or Surgah Formations) separate carbonates of Sarvak from Ilam Formation (Ghabeishavi et al., 2010).

The Sarvak Formation was deposited in a shallow carbonate shelf setting and its younger parts belong to shallower environments compared to older parts. According to Fig. 2, this formation overlies Kazhdumi Formation and its upper boundary is an unconformity, interpreted as uplift (Ghabeishavi et al., 2010).

In terms of lithology, the Sarvak Formation consists mainly of limestone and sometimes traces of dolomite. The microfacies and depositional reservoir quality of the Upper Sarvak Formation show a good relationship with depositional facies, so that diagenetic controls on permeability and porosity are also facies-controlled. The main diagenetic process in Sarvak Formation are the compaction, dissolution, calcitization, cementation, neomorphism, bioturbation, dolomitization and fracturing

Among all, dissolution and fracturing are the most important factors which have positive effect on reservoir quality and cause to develop four dominate pore types including: fracture, vuggy, moldic, and interparticle pores (Fig. 3).

3. Dataset

In this study data related to three wells of the Sarvak interval of studied oil field are used. Utilized well logs include Caliper, P-wave velocity (*Vp*), density log (RHOB), gamma ray (GR), and neutron density (NPHI) log (Fig. 4). The S-wave velocity (*Vs*) log is also estimated using Greenberg–Castagna limestone relationship. We incorporate the complete geological reports and core studies that have already been carried out by National Iranian Oil Company (NIOC) to verify the concluded results.

4. Methodology

4.1. Velocity-deviation log

The velocity-deviation log (VDL) is the difference of the real sonic log and the synthetic sonic log calculated from the porosity value estimated from time-average equation. The steps followed to calculate VDL is given in Appendix.

Using the deviation of this log to negative or positive values, the pore types can be distinguished as follow (Anselmetti and Eberli, 1999):

a) The positive velocity deviation: indicates zones in which velocity is higher than expected from the porosity values, caused by frame-forming pore types such as moldic or vuggy porosities.
b) Zero velocity deviation: indicates intervals with small positive or negative deviation from expected velocity obtained from time-averaging equation, such as interparticle porosity or microporosity.

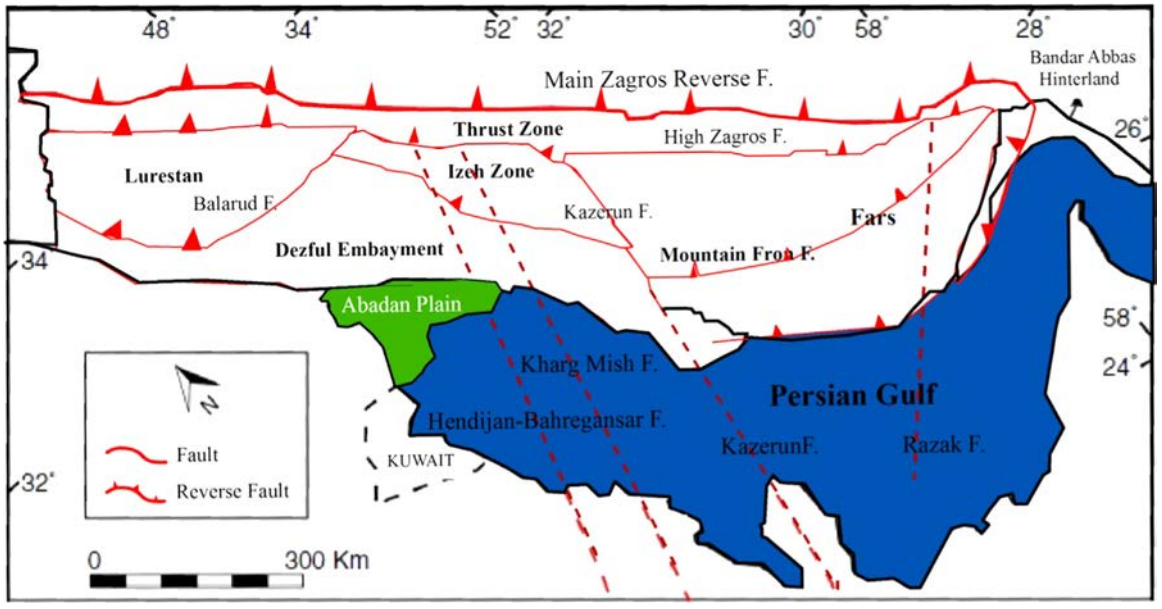

Fig. 1. The location of the Abadan Plain in the Zagros. Modified after Sherkati and Letouzey (2004).

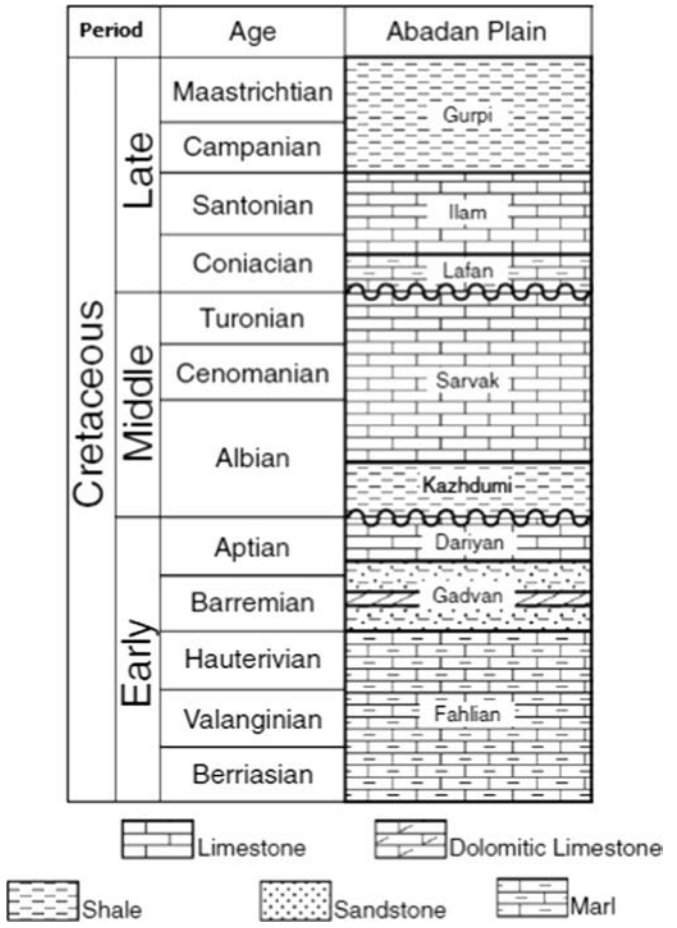

Fig. 2. The stratigraphy of the Cretaceous in the Abadan Plain (SW Iran). Modified after Bashari (2007a).

c) The negative velocity deviation: indicates zones in which sonic log velocities are unusually lower than expected from the porosity values. There are three possible explanations of this observation: caving or irregularities of the borehole wall, fracturing, high content of free gas.

4.2. Feature vector

To improve the precision of pore type identification a set of features is needed. In this study, the frame flexibility factor (γ), porosity, P-wave velocity, and S-wave impedance are used as a set of proper informative parameters.

4.2.1. The frame flexibility factor

In order to quantify the effect of pore structure changes on seismic wave velocity in carbonates, Sun (2000) defined useful elastic parameter called frame flexibility factor (γ). The frame flexibility factor is a rock physics parameter which depends less on porosity than wave velocity does and shows a good relationship to pore structure variation as well as solid/pore connectivity and grain size (Sun, 2004). This parameter can be obtained using equations given below (Sun, 2000):

$$\gamma = 1 + \frac{\ln(f)}{\ln(1-\varphi)} \tag{1}$$

$$f = \frac{1 - \left(\frac{K_f}{K_s} + \left(1 - \frac{K_f}{K_s}\right)\varphi\right)F_k}{(1-\varphi)\left(1 - \frac{K_f}{K_s}\right)F_K} \tag{2}$$

$$F_K = \frac{K_S - K}{\varphi(K_S - K_f)} \tag{3}$$

$$K = \left(V_P^2 - \frac{4}{3}V_S^2\right)\rho \tag{4}$$

where γ is the frame stiffness factor, K_s and K_f are matrix and fluid bulk moduli, respectively, and ϕ is porosity.

4.2.2. Velocity–porosity relationship

Pore geometry is the main controlling factor for acoustic properties and may dramatically affect the velocity–porosity trend in carbonate rocks. The complexity of carbonate pore types may cause rocks with equal porosity have very different velocities (Dou et al., 2011; Eberli et al., 2003). In general, it is found that frame-embedded pores, such as moldic and vuggy pores, tend to be rounded and resistant to pressure change, however, crack-like pores tend to be flat and will have much lower stiffness. As a result, a seismic wave propagates faster in rocks dominated by stiff pores than it does in rocks with small concentrations of cracks (Dou et al., 2011; Zhao et al., 2013). The dependency of the seismic wave velocity on pore type is so important that it can cause different pore types form clusters in the velocity–porosity diagram (Eberli et al., 2003). In other word, scattering velocity–porosity cross-plot at equal porosity is caused by the specific pore type and their resultant elastic property. Therefore, the velocity–porosity cross-plot can be regarded as an effective rock physics template to quantify the effect of volume fractions of different pore types on the elastic properties of carbonate rocks.

4.2.3. Impedance–porosity relationship

The main objective of reservoir seismic modeling is to relate a seismically-derived rock elastic property to quantitative petrophysical properties (Anselmetti and Eberli, 1993). The impedance–porosity relationship is a commonly used approach in evaluating reservoir porosity from acoustic impedance. Pore type variations in a carbonate rocks may result in a complicated Impedance–porosity relationship and there may be a big scattering at a given porosity. Since the pore structure can affect both compressional and shear wave velocities, the cross-plot of density porosity against shear wave impedance is used to characterize the effect of pore structure on acoustic velocity. the frame flexibility factor γ is also used to cluster the scattering samples at given porosity.

4.3. Parzen classifier

Parzen classifier is one of the most efficient non-parametric algorithm. The algorithm uses windowing approach to estimate the probability density function (pdf) and employs Bayes rule to assigns the most likely class to a given data. The Parzen classifier can be followed in 4 steps (Duda et al., 2002):

a) Normalizing all input data using:

$$X_i = \frac{x_i - \mu_i}{\sigma_i} \tag{5}$$

where x_i is the original data, X_i is its normalized form, σ_i and μ_i are the standard deviation and average of the same data respectively.

b) Specifying a hyper-space at center of x (i.e. the position of

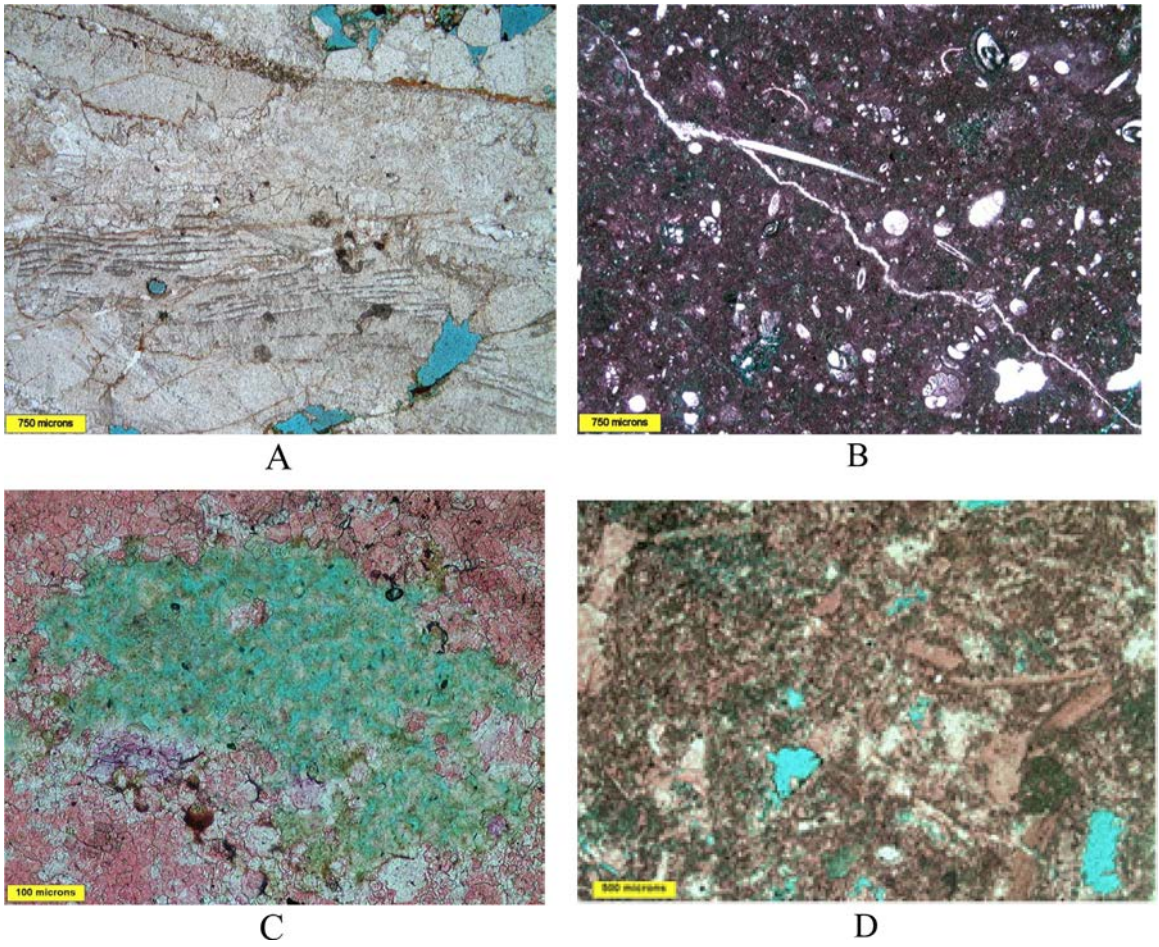

Fig. 3. Photomicrographs of prepared thin sections showing various pore types of reservoir. (a) Rudist grainstone with residual (primary) interparticle macroporosity. (b) Bioclastic mudstone/wackestone. sharp fracture runs across the field of view from top left to bottom right. (c) Vuggy microporosity occupied by Kaolinite. (d) Mouldic macropores.

test depth). The volume of the hyper-space is:

$$V_{\mathrm{n}}=h_{\mathrm{n}}^{\mathrm{d}} \tag{6}$$

c) Determining $p_{\mathrm{n}}(x)$ for each classes (zones) separately:

$$p_{\mathrm{n}}(x)=\frac{k_{\mathrm{n}}}{nV_{\mathrm{n}}} \tag{7}$$

where n illustrates the total number of samples belongs to a specific class in the training well. k_n is the number of trained samples in hyper-space, given by:

$$k_n=\sum_{i=1}^{n}\varphi\left(\frac{X-X_{\mathrm{i}}}{h_n}\right) \tag{8}$$

where φ is the window function or kernel in the D dimensional space.

d) The studied depth assigns to the class which has greater $p(x)$.

5. Results and discussion

5.1. Rock physics diagnostics application to Sarvak formation

Whole rock X-Ray Diffraction (XRD) analysis was carried out on 91 core samples in order to identify the mineralogy of rock-forming carbonates (calcite–dolomite) and other associated minerals such as quartz and clay minerals. Mineral composition of the studied Sarvak Formation interval dominantly consists of calcite (65%), dolomite (23%) with some clay. The basic parameters used for computing bulk modulus of the matrix were taken from core studies (Table 1).

The Voigt–Reuss–Hill mixing model is used to obtain the elastic moduli of the solid rock matrix.

The cross-plot of porosity versus frame flexibility factor is shown in Fig. 3. In terms of the frame flexibility factor (γ), the scattering points can be grouped into three clusters using different (γ) values (Fig. 5).

Low to medium negative (γ) values are related to the lithology intervals that mostly contain interparticle pores. Moldic/vuggy pores with high aspect ratio have medium (γ) values. The third pore type is fractures with a softer structure (low aspect ratio), having high values for (γ).

To determine the proper cutoffs for pore type classification, the inverted frame flexibility factor is calibrated to core data. Applying calibrated values, interparticle pores are classified by $\gamma<-1$, the (γ) values between -1 and $+1$ are the best class for moldic and vuggy pores, and finally fractures are classified by $\gamma>+1$.

Fig. 6 shows the cross-plot of P-wave velocity against porosity classified by (γ) value in well No. 1. It is evident that there is an inverse velocity–porosity relationship with a wide-scattered range at a given porosity. Samples of porosity $>20\%$, the porosity–velocity trend is more scattered than those samples in the lower porosity range. For example, samples of similar porosity of 10% have a velocity difference about 600 m/s but the velocity difference is $\sim$250 m/s at about 3% porosity.

In carbonate reservoir, the impedance–porosity relationships can be affected by pore structure (Dou et al., 2011).

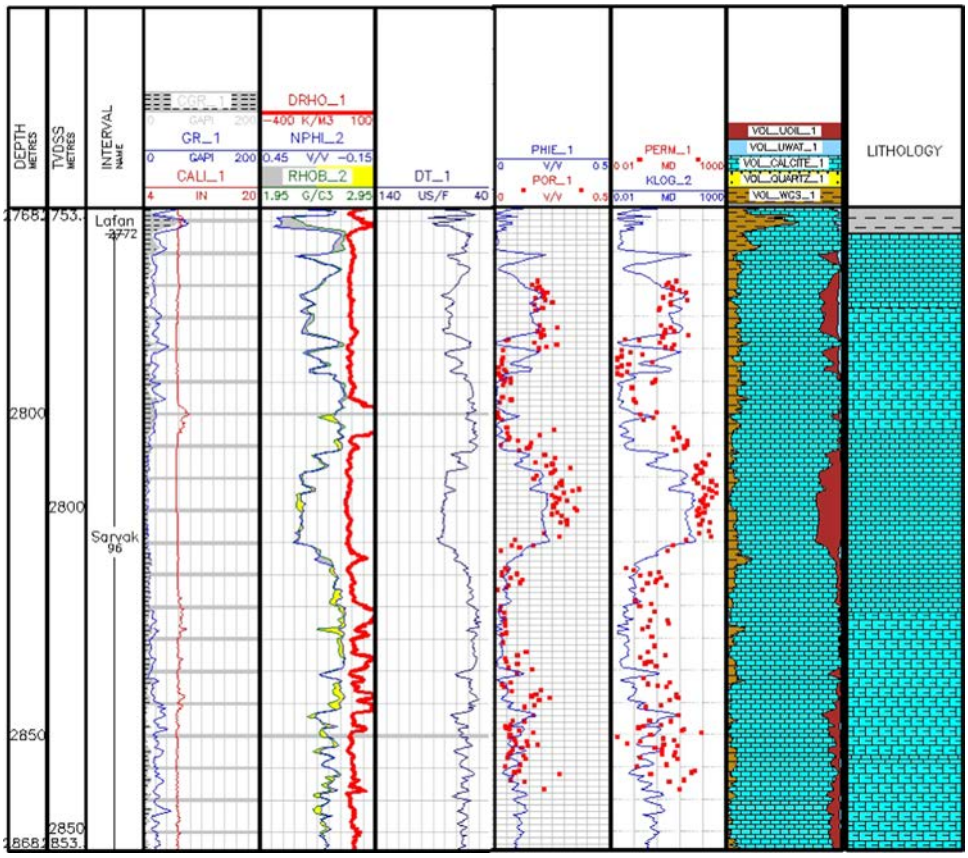

Fig. 4. Example of utilized well logs in well No.1 from Studied oil field, SW Iran.

Table 1
Main mineralogical components of the reservoir.

Minerals and fluid	Density (g/cc)	Bulk modulus (GPa)	Shear modulus (GPa)
Clay	2.56	20.8	7.5
Dolomite	2.85	84.10	45
Calcite	2.71	78	32
Oil	0.85	0.43	–
Water	1.14	3.05	–

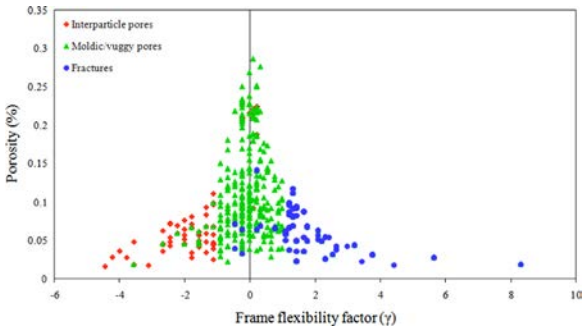

Fig. 5. Cross-plot of porosity–frame flexibility factor in well No.1.

Fig. 7 displays the cross-plot of density porosity against shear wave impedance, indicating a big scatters similar to P-wave velocity–porosity lines. Using a classified range of (γ), these lines are classified which indicates shear wave impedance–porosity relationship is affected by pore type and rock texture.

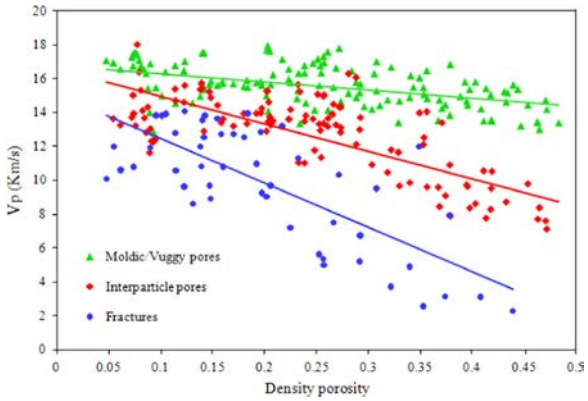

Fig. 6. P-wave velocity–porosity cross-plot in well No.1.

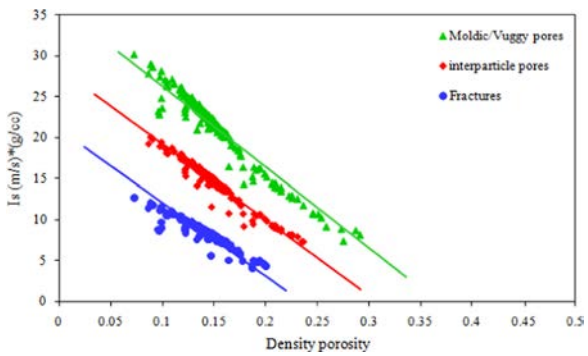

Fig. 7. Cross-plot of S-wave impedance against density porosity in well no.1.

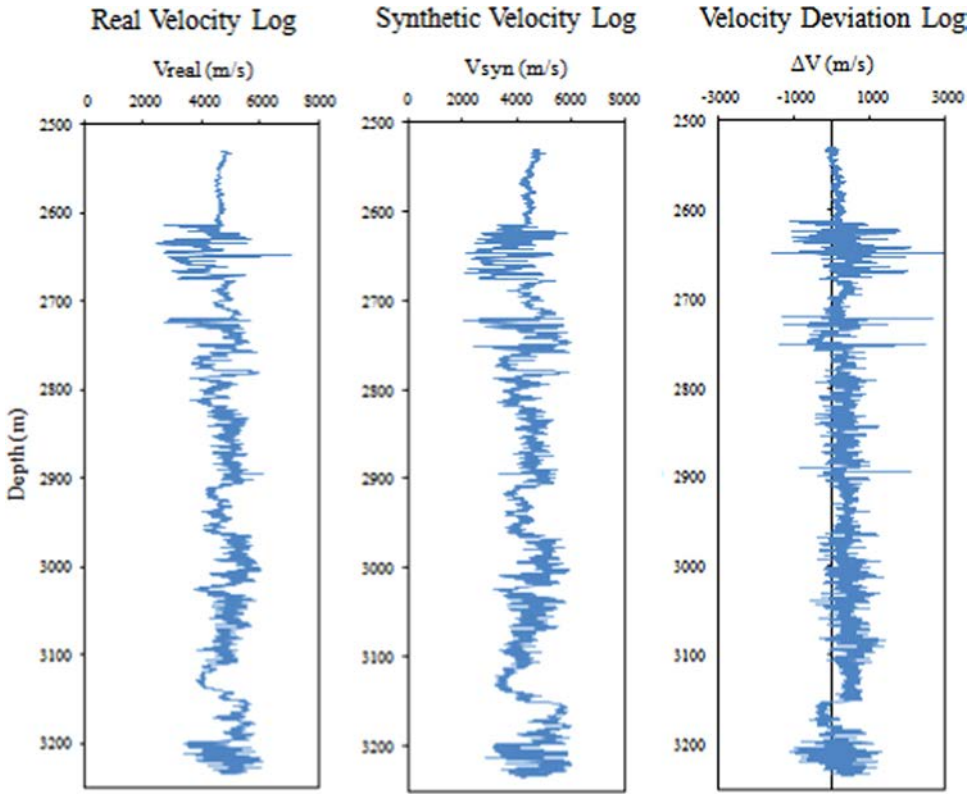

Fig. 8. Velocity deviation log in well No.1.

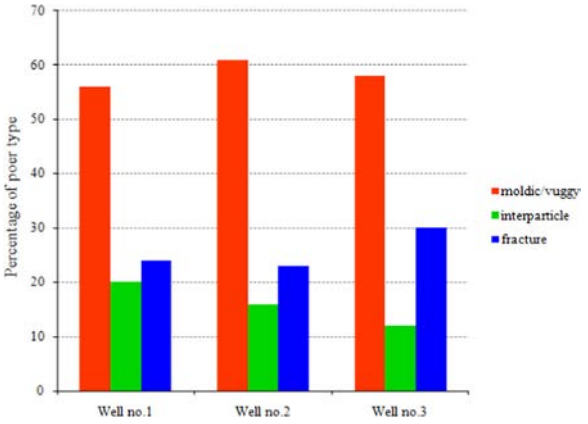

Fig. 9. Percentage of three defined pore types in each studied well resulted from VDL.

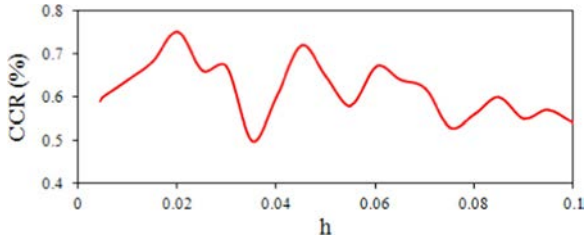

Fig. 10. Optimization of h value versus CCR in well No. 1. CCR reaches its maximum value at $h=0.02$.

5.2. Pore type characterization using velocity-deviation log

The velocity-deviation log is generated to determine the main pore types of reservoir under study (Fig. 8). As seen in the figure, there are 3 deviations in velocity-deviation log: large positive, zero and large negative deviations.

Large positive deviation ($\Delta V > +400$) represents relatively high velocities with regard to porosity, and caused mainly by moldic porosities. It covers 56% of studied interval in well No.1, 61% of studied interval in well No.2, and 58% of studied interval in well No.3.

Zero deviation ($-400 < \Delta V < +400$) indicates intervals dominated by interparticle pore type. It covers a total thickness of 142 m (20%) out of total thickness of 710 m in well No.1, 92 m (16%) out of total thickness of 574 m analyzed in well No.2, and 65 m (12%) out of the of 538 m analyzed in well No.3.

Large negative deviation ($\Delta V < -400$) indicates that other factors than lithology control the pore structure in the studied reservoir such as caving or irregularities of the borehole wall, high content of free gas, and fractures (Anselmetti et al., 1999). To be certain about which of the above mentioned factors is predominant, the generated velocity deviation log is correlated with density and caliper logs. In general, intervals with high content of free gas can increase density log and caving may cause caliper log give relatively high deflection. In the absence of these factors, the result of large negative velocity-deviation is due to the presence of fracture which is the case of this study.

Fig. 9 summarizes the percentage of each pore type in three studied wells based on generated VDL.

A coding system is used to discriminate the above mentioned deviations as follows: with respect to large positive deviation intervals with dominate moldic/vuggy porosities, this interval is coded by -1 (class 1). With respect to zero deviation intervals with dominate interparticle pores, this interval is coded by 0 (class 2). With respect to large negative deviation intervals with dominate fracture porosities, this interval is coded by $+1$ (class 3).

Table 2
Results of Parzen classifier in three studied wells.

Well No.	1	2	3
Confusion matrix	0. 86 0. 11 0. 03 [0. 18 0. 78 0. 04] 0. 17 0. 21 0. 62	0. 81 0. 19 0 [0. 17 0. 80 0. 03] 0. 12 0. 15 0. 73	0. 83 0. 15 0. 02 [0. 12 0. 78 0. 1] 0. 19 0. 12 0. 69
Trace of Confusion matrix	2.26	2.34	2.3
Classification correctness rate (%)	75.3	78	76.7
Optimum h	0.02	0.01	0.01

5.3. Classification result

The Parzen classifier with the selected feature set has been applied to available dataset related to three wells of the Sarvak Formation and defined pore types are identified in each well separately. For each individual well, the classifier is trained against 70% of the randomly selected data points and its accuracy in identifying desired classes is tested by the remaining 30%. Confusion matrix is used to show the results of classification process. To determine the efficiency of the classifier, Classification Correctness Rate (CCR) is computed by dividing the trace of confusion matrix by number of classes.

The window size related to the Parzen classifier (i.e. h) is optimized through measuring the CCR for different h values. The optimum h value is the one that generates the highest CCR. Fig. 10 shows the plot of the CCR versus h in well No.1. As it can be seen in the figure, 0.02 is optimum h value which maximizes the confusion matrix trace to 2.26.

The results of classification in testing intervals of three studied wells are shown in Table 2. In this table, trace of confusion matrix, CCR, and optimum h value are given in separate rows.

According to the table, the accuracy of Parzen classifier varies from 75.3% to 78% (average accuracy of 76.7%) which exhibits an acceptable capability in identifying defined pores in studied wells. This gives an average accuracy of 82.7%, 78.7%, and 68.3% for interparticle, moldic/vuggy, and fracture pore types classification respectively.

Comparing to interparticle or fracture pore types, identifying moldic/vuggy pores is much more accurate in terms of classification accuracy. This probably happens due to the dependency of Parzen classifier on the amount of training data. For example, referring to the Fig. 8, it can be seen that the percentage of moldic/vuggy interval in well No.1 is greater than other types and therefore the percentage of misclassification for this class (16.7% on average) is less than that of interparticle or fracture pores. These results indicate that the proposed data-driven algorithm can be successfully used to identify pore types in studied carbonate reservoir through selected rock physics features.

6. Conclusion

Heterogeneity of carbonate rocks is a complicated function of several parameters such as mineral composition, pore fluid, and pore structure, due to some post-diagenesis process. Variation in pore type as the most important parameter cause complexity in the elastic behavior of carbonate rocks that result in ambiguous seismic responses of the reservoir.

In this paper, we proposed a new algorithm to evaluate and identify three desired pore types (i.e. interparticle, moldic/vuggy, and fracture) in a carbonate reservoir based on rock physics modeling. The algorithm was applied to a dataset related to three wells of an oil field located in southwest of Iran. The results obtained from applying the algorithm can be listed as follows:

- Employing the velocity-deviation log (VDL) three dominant pore types of reservoir under study were identified as: Large positive deviation ($\Delta V > +400$) which indicates vugg/moldic porosities, Zero deviation ($-400 < \Delta V < +400$) that indicates intervals dominated by interparticle pore type, and Large negative deviation ($\Delta V < -400$) which indicates the presence of fracture.
- Using the frame flexibility factor (γ), moldic/vuggy porosities can be identified by γ values between -1 and $+1$. Interparticle pores are classified by $\gamma < -1$, and fractures are classified by $\gamma > +1$.
- Identified pores make specific clusters to gathers in cross-plot of velocity–porosity as well as impedance–porosity which can be used as proper input features for classification process.

Using the selected features, three dominant pores were identified through Parzen classifier with average accuracy of 76.7% and reveal that the proposed algorithm is efficiently capable to identify the dominate pore type in studied carbonate reservoir.

Appendix A. The velocity-deviation log (VDL)

The velocity-deviation log (VDL) which can be obtained by combining the sonic log with the neutron-porosity log is a useful tool for characterizing the predominant pore types and fractures in carbonate reservoir rocks. Since the presence of shale in formations can influence the response of the neutron porosity log, the shale volume is first estimated from gamma ray log by the following method:

$$V_{sh}=\frac{GR_{log}-GR_{min}}{GR_{max}-GR_{min}} \tag{A1}$$

where GR_{log} is the gamma ray reading of the formation, GR_{max} and GR_{min} are the maximum and the minimum gamma ray, respectively.

Therefore the shale corrected neutron porosity (φ_{Nshc}) is:

$$\varphi_{Nshc}=\varphi_N-V_{sh}\times\varphi_{Nsh} \tag{A2}$$

where φ_N is the porosity read by neutron log, V_{sh} is the shale volume and φ_{Nsh} is neutron log reading in shaly formation.

Similar to neutron porosity, the shale corrected neutron porosity (φ_{Dshc}) is:

$$\varphi_{Dshc}=\varphi_D-V_{sh}\times\varphi_{Dsh} \tag{A3}$$

Having Eq. (2) and (3), the neutron-density log can be obtain using the equation given bellow:

$$\varphi_{ND}=\sqrt{\frac{\varphi_{Nsh}^2+\varphi_{Dsh}^2}{2}} \tag{A4}$$

Substituting φ_{ND} in sonic porosity equation will results in:

$$\varphi_{ND}=\frac{DT_{syn}-DT_{ma}}{DT_{fl}-DT_{ma}} \tag{A5}$$

where DT_{syn} is the synthetic transient time log, DT_{ma} and DT_{fl} are the matrix and pore fluid transit times, respectively.

The Velocity-Deviation Log (VDL) can then be obtained through:

$$\Delta V_p = V_{p_{real}} - V_{p_{syn}} = \frac{304.8}{DT_{real}} - \frac{304.8}{DT_{syn}} \quad \text{(A6)}$$

References

Adam, L., Batzle, M., Brevik, I., 2006. Gassmann's fluid substitution and shear modulus variability in carbonates at laboratory seismic and ultrasonic frequencies. Geophysics 71, F173–F183.

Anselmetti, F.S., Eberli, G.P., 1993. Controls of sonic velocity in carbonates. Pure Appl. Geophys. 141, 287–323.

Anselmetti, F.S., Eberli, G.P., 1999. The velocity-deviation log: a tool to predict pore type and permeability trends in carbonate drill holes from sonic and porosity or density logs. Am. Assoc. Pet. Geol. Bull. 83 (3), 450–466.

Assefa, S., McCann, C., Sothcott, J., 2003. Velocities of compressional and shear waves in limestones. Geophys. Prospect. 51, 1–13.

Avseth, P., Mukerji, T., Mavko, G., Dvorkin, J., 2010. Rock-physics diagnostics of depositional texture, diagenetic alterations, and reservoir heterogeneity in high-porosity siliciclastic sediments and rocks – a review of selected models and suggested work flows. Geophysics 75, A31–A47.

Baechle, G.T., Eberli, G.P., Wegar, R.J., Massaferro, L., 2009. Changes in dynamic shear moduli of carbonate rocks with fluid substitution. Geophysics 74, E135–E147.

Bashari, A., 2007a. Integrated 3D seismic and petrophysical data of the Sarvak formation in the Persian Gulf. First Break 25, 45–53.

Bracco, G.L., Gartner, P.D., Wagner, G.T., Baechle, Y.F., Sun, R., Weger, G.P., Eberli, W., Asyee, H., illgartner, K., Van der Kolk, J., Leguijt, M.R., Nasser, J., Massaferro, 2005. Obtaining permeability from seismic data: a new breakthrough in carbonate reservoir modeling. In: Proceeding of the International Petroleum Technology Conference, p. 10577.

Dou, Q., Sun, Y.F., Sullivan, C., 2011. Rock-physics-based carbonate pore type characterization and reservoir permeability heterogeneity evaluation, upper San Andres reservoir, permian basin, West Texas. J. Appl. Geophys. 74, 8–18.

Duda, R.O., Hart, P.E., Stork, D.G., 2002. Pattern Classification, 2nd ed. Wiley, New York.

Eberli, G.P., Baechle, G.T., Anselmetti, F.S., Incze, M., 2003. Factors controlling elastic properties in carbonate sediments and rocks. Lead. Edge 22, 654–660.

Fournier, F., Leonide, P., Biscarrat, K., Gallois, A., Borgomano, J., Foubert, A., 2011. Elastic properties of microporous cemented grainstones. Geophysics 76, E211–E226.

Ghabeishavi, A., Vaziri-Moghaddam, H., Taheri, A., Taati, F., 2010. Microfacies and depositional environment of the cenomanian of the bangestan anticline SW Iran. J. Asian Earth Sci. 37, 275–285.

Mahbaz, S.B., Sardar, H., Memarian, H., 2012. Determination of rock physics model for the carbonate fahliyan formation in two oil wells in southwestern Iran. Explor. Geophys. 43, 47–57.

Matonti, C., Guglielmi, Y., Viseur, S., Bruna, P.O., Borgomano, J., Dahl, C., Marié, L., 2014. Heterogeneities and diagenetic control on the spatial distribution of carbonate rocks acoustic properties at the outcrop scale. Tectonophysics 638, 94–111.

Pyrcz, M.J., Deutsch, C.V., 2014. Geostatistical Reservoir Modeling. Oxford University Press, p. 448.

Sherkati, S., Letouzey, J., 2004. Variation of structural style and basin evolution in the central zagros (Izeh zone and dezful embayment). Iran Mar. Pet. Geol. 21, 535–554.

Sun, Y.F., Core-log-seismic integration in hemipelagic marine sediments on the eastern flank of the Juan De Fuca Ridge. In: Proceedings of Ocean Drilling Program Science Results. 168, 2000, pp. 21–35.

Sun, Y.F., 2004. Effects of pore structure on elastic wave propagation in rocks AVO modeling. J. Geophys. Eng. 1, 268–276.

Wang, Z., Wang, R., Weger, R., Li, T., Wang, F., 2015. Pore-scale modeling of elastic wave propagation in carbonate rocks. Geophysics 80 (1), D51–D63. http://dx.doi.org/10.1190/geo2014-0050.1.

Xu, S., Payne, M.A., 2009. Modeling elastic properties in carbonate rocks. Lead. Edge 28, 66–74.

Zhao, L., Nasser, M., Han, D., 2013. Quantitative geophysical pore-type characterization and its geological implication in carbonate reservoirs. Geophys. Prospect. . http://dx.doi.org/10.1111/1365-2478.12043